

Uhandisi Journal, Vol.8, no.1, 1984

NEGATIVE CORONA CURRENT CHARACTERISTICS OF AN ELECTRIC WIND SYSTEM

By

Kadete, H.¹

ABSTRACT

The corona current characteristics of an electric wind system are investigated. First a brief summary of the negative point to plate corona mechanism and characteristics are presented. Then empirical equations for corona currents of an electric wind system are derived. Current waveform characteristics are also discussed. The effects of placing parallel rods in between a point-plate electrode gap to the corona currents are highlighted.

INTRODUCTION

It is generally known that forced convection due to an electric wind enhances the rate of heat transfer across a solid gaseous interface. This results from the modification of the natural convection currents and is possibly due to the disruption of the thermal boundary layer (1-5). For this purpose, an electric wind is usually created by applying a negative d.c. voltage across an inhomogeneous electrode configuration such as a point-plate or a wire-plate arrangement. The application of corona as a means of creating an electric wind is well treated by Chattock (6), Loeb (7), (8), and Robinson (9). The operating characteristics of a non-familiar electric wind system which employs a multitooth comb as the cathode with two parallel grounded rods as the anode are determined. Such an electrode configuration permits the placement of a heat transfer surface behind the rods. If this is a flat plate or a cylinder or any other grounded electrically conducting object, it means that a three electrode system has been realised employing the heat transfer surface, as the third electrode. With such a configuration, the operating characteristics of the wind system may be modified by changes in the position of the electrodes.

¹ Faculty of Engineering, University of Dar es Salaam

Negative corona mechanism and characteristics

Negative corona phenomena have been intensively studied experimentally. A very extensive treatment of its mechanism and characteristics can be found in books such as by Loeb (8), Cobine (10), Nasser (11), and a host of many others. A good summary of negative corona characteristics for a point-plate electrode configuration can be found in a paper by Lama (12).

Depending on gap length and voltage across it, the corona discharge is normally pulsating or a continuous glow around the discharge point. On raising the voltage, the transition from a pulsating discharge referred to as Trichel pulses to a continuous glow then to sparkover will take place for longer gap lengths whilst for shorter gap lengths the transition will be from Trichel pulses discharges directly to sparkover. For even shorter gap lengths there is sparkover directly whenever breakdown occurs.

Four distinct regions of the discharge can be identified at the cathode, namely, the Crookes dark space, the negative glow, the Faraday dark space and the positive column.

A model of the Trichel pulse formation was developed by Loeb (8). In time sequence, the pulse is initiated by an electron ejected from the cathode surface by some mechanism such as field emission or positive ion bombardment, and proceeds by Townsendian ionization. The positive ions left in the wake of the electron avalanche serve to increase the ionization field, leading to a rapid build up of the current. The positive ions further provide an additional source of electrons through bombardment of the cathode surface. The electron avalanche is choked off in a very short time by the negative space charge which forms by electron attachment just outside the ionization region and reduces the field in that region below the avalanche threshold. The rise time of the pulse is extremely short, in the order of 10^{-9} sec.

The electron avalanche then remains off until the negative space is removed by the electric field a sufficient distance, referred to as the "clearing distance" the time interval involved is correspondingly referred to as the "clearing time", for the field to regain its critical value.

Well known empirical relationships governing Trichel pulses are:

1. The time averaged corona current, I , and the Trichel pulse repetition rate, F , are linearly related for a given electrode configuration, and the proportionality constant is the charge per pulse, Q .

$$I = QF.$$

(1)

2. The charge per pulse depends on the shape of the discharge point. If the discharge electrode is a hemispherical cap, for example, then Q , is a certain function of the cap radius.

It follows therefore that

$$Q = f_1(r), \quad (2)$$

3. The current repetition rate, F , and hence the time averaged current, I , is directly proportional to the voltage above threshold ($U-U_0$), where U_0 is the corona onset voltage. That is,

$$I \propto F \propto (U - U_0) \quad (3)$$

It is well known that, at certain well separated values of voltage, a sudden change in repetition rate, F , charge per pulse, Q , and therefore, I , could occur.

4. At constant corona current, I , the repetition rate, F , is independent of the gap length, S , but it is dependent on the form or shape of the discharge point, for a hemispherical cap it may be said that

$$I = f_2(r). \quad (4)$$

If no sparking intervenes, a continuous glow is formed when the Trichel pulses nearly merge in time. A typical Trichel current pulse waveform has a very fast rise time, reaches the maximum, is followed by a fast fall time then stabilizes to a flat plateau, after which it obtains a rather fast fall time and when its value is nearly zero it decays very slowly (13), (14).

The fast rise time and high amplitude of the Trichel pulse current waveform is due to the motion and avalanche growth of the electrons in the high field region around the cathode, the rest of the Trichel pulse current waveform is determined by the slower motion of the heavy negative ions formed after the attachment of the electrons to the air molecules. This part of the motion takes place in the low electric field region of the gap spacing.

The electric wind system and test circuits

The discharge point is a 15-tooth stainless steel comb as shown in fig.1.a. Each tooth being a 90° edge.

For the determination of corona current waveforms it was necessary to use a comb with one tooth so that clear oscillograms of current pulses could be obtained - see fig. 1.b.

The anode consists of two parallel stainless steel rods of 5 mm diameter each. The heat transfer surface is a flat stainless steel plate. When this is grounded, it acts as an extra anode electrode.

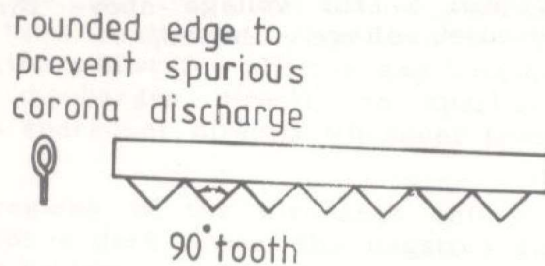


Fig. 1.a. The discharge electrode.



Fig. 1.b. The single tooth discharge electrode which was used in determining corona current waveforms.

A negative high voltage was applied at the discharge electrode by a Wallis type D.C. supply rated at 0 - 30 kVDC, 0 - 1 mA, via a 2 M Ω current limiting resistor.

A 4000 pF, 20 kVDC, smoothing capacitor was connected in parallel with the DC supply circuit. Measurement of voltage was done by a highly sensitive electrostatic voltmeter (ESV) with four voltage ranges, 0 - 5, 0 - 10, 0 - 25 and 0 - 50 kV. Measurements of time averaged corona currents was performed by sensitive Keithley electrometers A₁ and A₂, type 610B and 610C having current ranges varying from 3 - 10⁻¹⁴ A. The current meters were connected in the ground circuits of the anodes as shown in fig. 1.c.

The determination of corona current waveforms in the grounded anode circuit was performed by measuring the voltage waveforms across the $10\text{ k}\Omega$ resistors. These voltages were fed into the input stages of a dual beam Tektronix Oscilloscope type 556 having a frequency response of $0 - 20\text{ MHz}$. The input coaxial cable to the oscilloscope had a characteristic impedance of $50\ \Omega$, which meant that parallel to the $10\text{ k}\Omega$ measuring resistor a capacitance of $1 \times 100\text{ pf}$ was present, where l is the length of cable - see fig. 1.d. In this case $l = 2\text{ m}$.

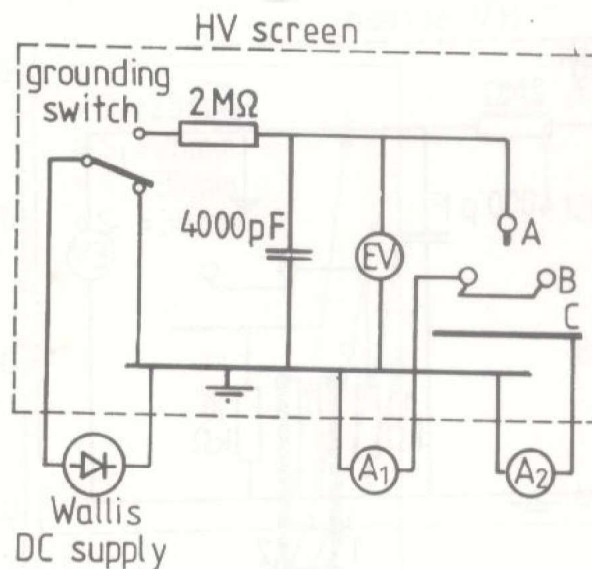


Fig. 1.c. Electric wind generator system showing experimental circuit for the determination of negative corona DC currents.

A = discharge electrode, B = two parallel rod connected to ground,
C = flat plate.

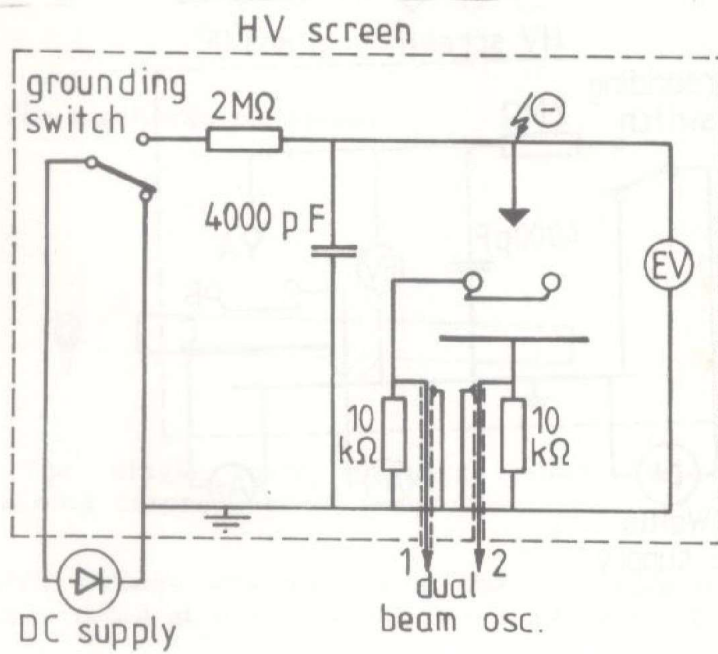


Fig. 1.d. Electric wind generator system showing experimental circuit for the determination of corona current waveforms.

Experimental results: rod corona current I_1

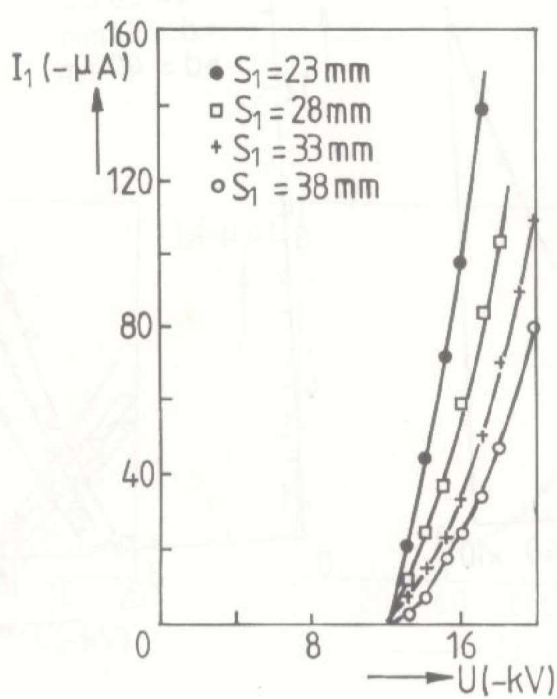
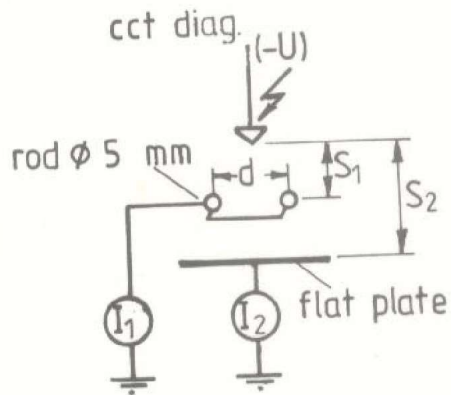


Fig. 2: Plots of I_1 vs U
 $d = 10$ mm.
 $S_2 = 83$ mm.

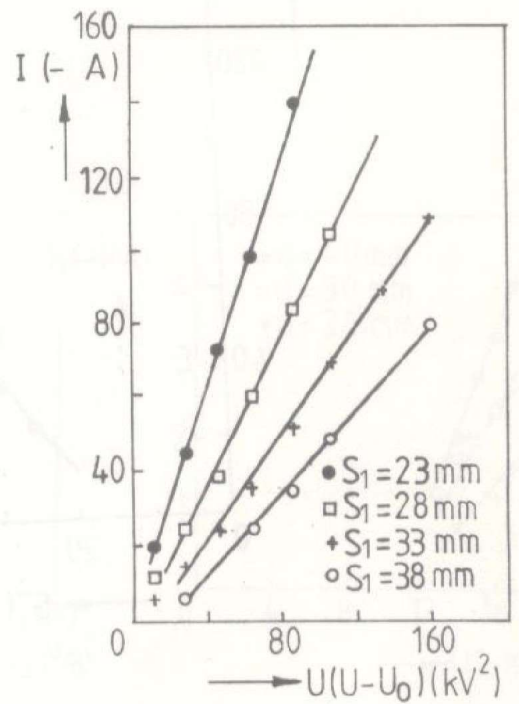


Fig. 3: Plots of I_1 vs $U(U-U_0)$.
 U_0 is determined from
 extrapolations of
 curves in Fig.2

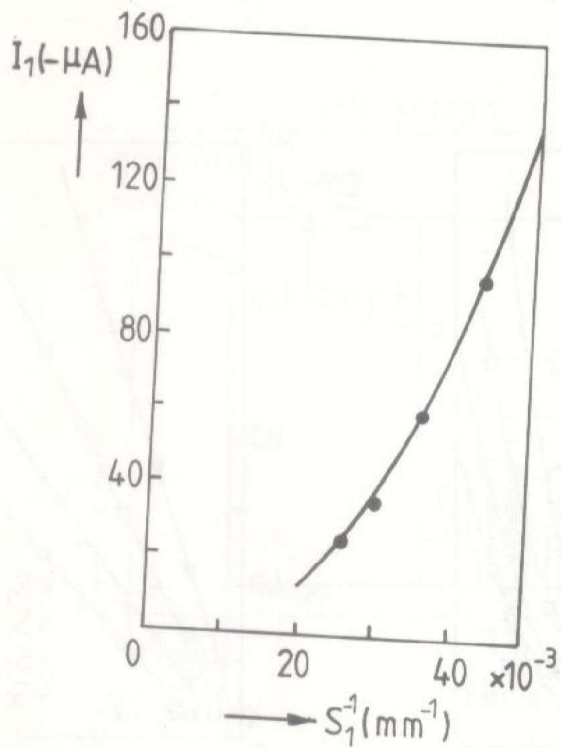


Fig.4: Plots of I_1 vs S_1^{-1} at a fixed value of U , d and S_2 , derived from Fig.2.

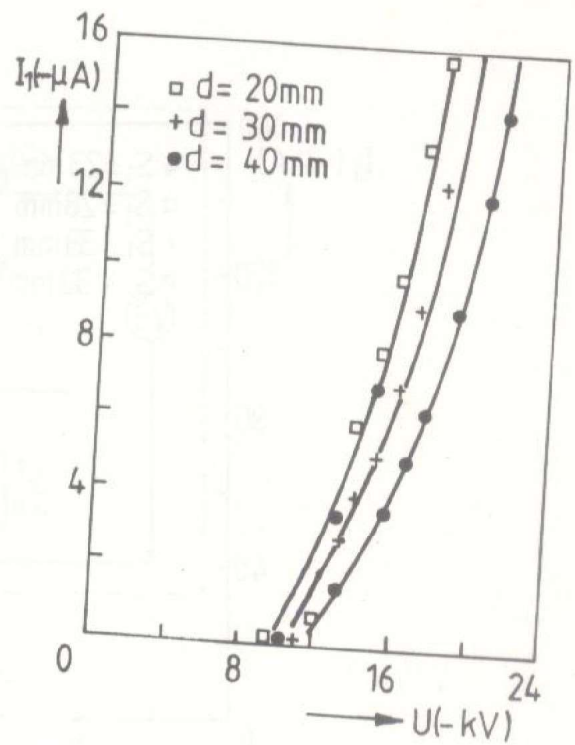


Fig.5 Plots of I_1 vs Voltage for various values of d with fixed S_1 and S_2 . The discharge electrode had only one tooth. $S_1 = 36\text{mm}$, $S_2 = 49\text{mm}$.

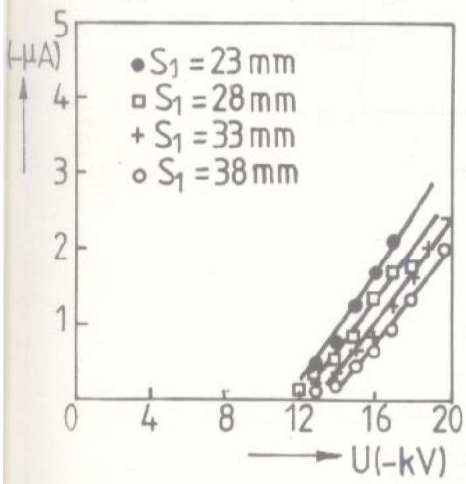


Fig. 6: Plots of I_2 vs U for different S_1 . Fixed $S_2 = 83\text{mm}$ and fixed $d = 10\text{mm}$

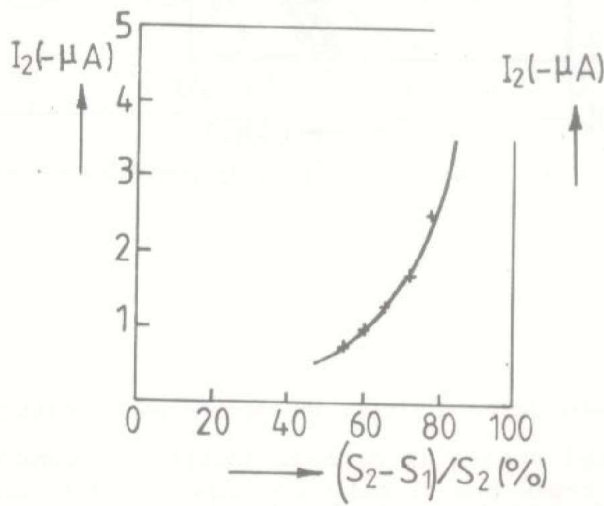


Fig. 7: Plots of I_2 vs $(S_2 - S_1)/S_2$. For a fixed value of voltage derived from Fig. 6. Fixed d, S_2, U .

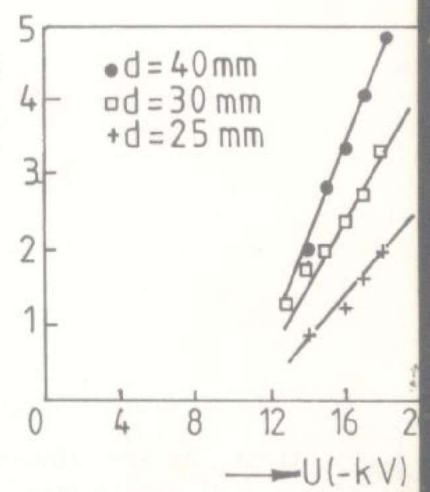


Fig. 8: Plots of I_2 vs U for different values of d . S_1 and S_2 are fixed. The discharge electrode had only one tooth. $S_1 = 36\text{mm}$, $S_2 = 49\text{mm}$.

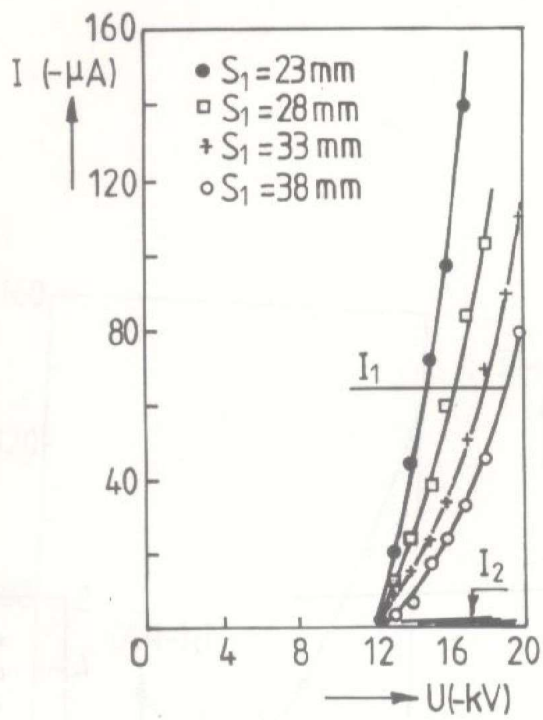


Fig.9: Plots of I_1 and I_2 vs U for fixed d , fixed $S_2 = 83\text{ mm}$ and varying $S_1 = d = 10\text{ mm}$.

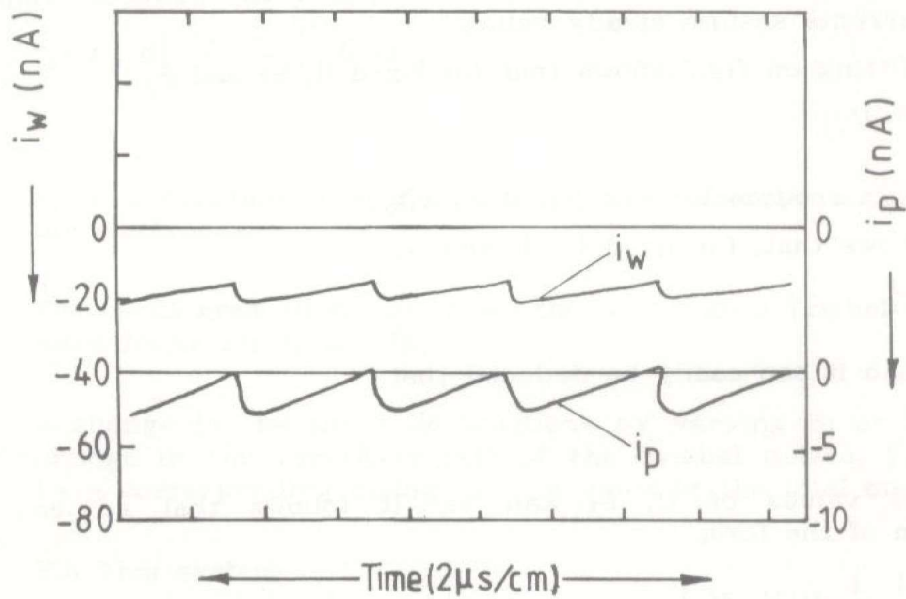


Fig. 10: Corona current waveforms of electric wind system.

The discharge electrode used in this case has only one 90° tooth - fig. 1.b. Upper beam indicates I_1 and lower beam shows I_2 .

Upper scale: vertical = 0.2 V/cm , horizontal = $2 \mu\text{s/cm}$, measuring resistor = $10 \text{ k } \Omega$

Lower scale: vertical = $.05 \text{ V/cm}$, horizontal = $\mu\text{s/cm}$, measuring resistor = $10 \text{ k } \Omega$.

Different oscillograms indicated that, for a constant Q , charge per pulse I_1 and $I_2 \propto f \alpha (V - V_0)$.

Discussion of experimental results

1. Corona current measurements indicated that corona current flows between discharge electrode and plate first. Increasing the gap voltage results in corona current, I_1 , flowing. From Fig. 6, I_2 depicts a linear relationship with the gap voltage, U , while I_1 shows a parabolic relationship with U , as is shown by fig.2.

Both values of I_1 and I_2 are non steady at and around corona inception. The dce meters, will typically be kicking and oscillating, displaying the sporadic behaviour of I_1 and I_2 . However voltages, both currents assume steady values.

2. Curve fitting on fig.2 shows that for fixed d , S_2 and S_1

$$I_1 \propto U(U - U_0)$$

which is a relationship confirmed by fig.3.

3. Fig.4 shows that, for fixed U , d , and S_2

$$I_1 \propto 1/S_1^2$$

4. From fig.5 it can easily be deduced that

$$I_1 \propto 1/d$$

at fixed values of U , S_1 and S_2 . It follows that an empirical equation of the form.

$$I_1 = k_1 \cdot \frac{1}{d} \cdot \frac{1}{S_1^2} \cdot U(U - U_0)$$

(5)

describes the functional dependence of I_1 on the gap voltage U , gap length S_1 , and rod spacing d .

k_1 is a constant which depends on the physical dimensions and form of the electrodes.

5. $I_2 \propto (U - U_0)$

for fixed values of S_1 , S_2 and d .

6. From fig. 7, it can be easily shown that

$$I_2 \propto \left(\frac{S_2 - S_1}{S_2} \right)^2$$

at a constant U and d .

7. The plot of fig.8 shows that

$$I_2 \propto d$$

at a constant U , S_1 and S_2 .

This leads to the following expression for the plate corona current,

$$I_2 = k_2 \cdot d \left(\frac{S_2 - S_1}{S_1} \right)^2 (U - U_0)$$

(6)

k_2 is a constant dependent on the physical shape and dimensions of the electrodes.

The oscillogram of fig.10 shows the well known Trichel pulse current wave forms for I_1 and I_2 .

A change in the electrode positions by varying S_1 or d results in a change in the repetition rate of the Trichel pulses, F , accompanied by a corresponding change in the value of the total current, I_T .

For this system.

$$I_T = I_1 + I_2$$

(7)

If the change is an increase of I_T then the higher value of F , was observed. That is the electrode configuration can be modified by changing d , S_1 or S_2 so that F is varied, moreover $I_T \propto F \alpha (U - U_0)$.

CONCLUSIONS

1. By making the gap electric field more inhomogeneous, hence increasing the Trichel pulse repetition rate, F , the rods serve to increase the total discharge current of a point plate electrode by multiples of up to 100's - see fig. 9.
2. The corona current to the plate, I_2 , and therefore to the heat transfer surface is reduced by the introduction of the rods in between the point and the plate. Its magnitude is in the range of 1 - 5 percent of the total corona current I_r .
3. The approximate functional dependence of corona currents I_1 and I_2 on the physical dimensions of the corona wind system and gap voltage are given by equations 5 and 6.
4. I_1 possesses the typical Trichel pulse waveform structure. It was observed from oscillograms that

$$I_1 \propto F \alpha U - U_0$$

REFERENCES

1. O'BRIEN, R.J. and A.J. Shine, "Effects of an Electric Field on Heat Transfer from a Vertical Plate in Free Convection", Transactions of the ASME-Journal of Heat Transfer, pp. 114-116, February, 1967.
2. FRANKE, M.E., "Effect of Vortices Induced by Corona Discharge on Free Convection Heat Transfer from a Vertical Plate", Transactions of the ASME-Journal of Heat Transfer, pp.427-432, August, 1969.
3. ASAKAWA, Y., "Promotion and Retardation of Heat Transfer by Electric fields", Nature, Vol. 261, pp. 220-221, 1976.
4. MORGAN, V.T. and R. Morrow, "Cooling of a Heated Cylinder in Still Air by Electrical Corona", Electrical Transactions - The Institution of Engineers, Australia, pp. 1 - 5, 1980.
5. KONNO, H. et al, "Heat Transfer from a Horizontal Fine Wire and Cylinders in a Corona Wind", Kagaku Kogaku Ronbushu (English translation), Vol. 7, pp. 343 - 348, 1981.

6. CHATTOCK, A.P., "On the Velocity and Mass of the Ions in the Electric Wind in Air", Philosophical Magazine, Vol, 48, No. 294, pp. 401-420, Nov., 1899.
7. LOEB, L.B., Fundamentals of Electricity and Magnetism, Wiley: Chapman & Hall, pp. 192-194, 1955.
8. LOEB, L.B., Electrical Coronas, University of California press, Berkeley, 1965.
9. ROBINSON, M., "Movement of Air in the Electric Wind of Corona Discharge", AIEE Trans., Vol. 114, Part I, Communications and Electronics, pp. 143-150, May, 1961.
10. COBINE, J.D. Gaseous Conductors, New York, Dover publications, Inc., 1958.
11. NASSER, E., Fundamentals of Gaseous Ionization and Plasma Electronic, New York, Wiley-Interscience, 1971.
12. LAMA, W.L. and C.F. Gallo, "Systematic Study of the Electrical Characteristics of the Trichel Current Pulses from Negative needle-to-plane Coronas", Journal of Applied Physics, Vol. 45, No.1, pp. 103-113, January, 1974.
13. MEEK, J.M. and J.D. Craggs, Electrical Breakdown of Gases, New York, Wiley & Sons, Inc., 1978.
14. GOLDMAN, M. and R.S. Sigmond, "Corona and Insulation" IEEE Transactions on Electrical Insulation, Vol. EI-17 No.2, pp, 90-105, April, 1982.